EUROPEAN ORGANIZATION FOR NUCLEAR RESEARCH

CERN-PPE/96-198
December 19, 1996

Measurement of $D_s^- \to \tau^- \bar{\nu}_\tau$ and a new limit for $B^- \to \tau^- \bar{\nu}_\tau$.

L3 Collaboration

Abstract

Using a data sample of 1,475,000 $Z \to q\bar{q}(\gamma)$ events collected during 1994 with the L3 detector at LEP, we have studied the purely leptonic decays of heavy flavour mesons, $D_s^- \to \tau^- \bar{\nu}_\tau$ and $B^- \to \tau^- \bar{\nu}_\tau$. A signal is observed in the invariant mass distribution $M(\gamma D_s^-)$ corresponding to the decay sequence $D_s^{*-} \to \gamma D_s^-$, $D_s^- \to \tau^- \bar{\nu}_\tau$, $\tau^- \to l^- \bar{\nu}_l \nu_\tau$. The branching fraction for $D_s^- \to \tau^- \bar{\nu}_\tau$ decays is measured to be $\mathcal{B}(D_s^- \to \tau^- \bar{\nu}_\tau) = 0.074 \pm 0.028(\text{stat}) \pm 0.016(\text{syst}) \pm 0.018(\text{norm})$. No signal of $B^- \to \tau^- \bar{\nu}_\tau$ decays is observed in the data, corresponding to an upper limit on the branching fraction $\mathcal{B}(B^- \to \tau^- \bar{\nu}_\tau) < 5.7 \times 10^{-4}$ at 90% CL.

Submitted to *Phys.Lett. B*

1 Introduction

Purely leptonic decays of heavy mesons are of particular interest due to their sensitivity to meson decay constants, which relate the absolute rate of various heavy-flavour transitions to CKM matrix elements. There exist several theoretical predictions for the decay constants f_D, f_{D_s} and f_B [1]; the agreement between the different approaches, however, is not very good. Therefore, the measurement of the Cabibbo-favoured process [1)] $D_s^- \to \ell^- \bar{\nu}_\ell$, the easiest to access experimentally, can help discriminate among the different theoretical models.

In the Standard Model the width of the decay $D_s^- \to \ell^- \bar{\nu}_\ell$ is predicted to be

$$\Gamma(D_s^- \to \ell^- \bar{\nu}_\ell) = \frac{G_F^2 \, f_{D_s}^2 \, |V_{cs}|^2 \, M_\ell^2 \, M_{D_s}}{8\pi} \, (1 - \frac{M_\ell^2}{M_{D_s}^2})^2 \, , \qquad (1)$$

where G_F is the Fermi coupling constant, M_{D_s} and M_ℓ are the particles masses, f_{D_s} is the decay constant and V_{cs} is the CKM matrix element.

Measurements of the leptonic decays $D_s^- \to \mu^- \bar{\nu}_\mu$ have been reported by several experiments [2–4]. The observation of $D_s^- \to \tau^- \bar{\nu}_\tau$ decays has been reported by BES [5]. The branching fraction $\mathcal{B}(D_s^- \to \tau^- \bar{\nu}_\tau)$ is expected to be $0.0485 \times (f_{D_s}/250 \text{ MeV})^2$ according to Equation 1. Since f_{D_s} is expected to be in the range 200-300 MeV, this decay could be accessible at LEP.

Similarly, within the Standard Model, the branching fraction $\mathcal{B}(B^- \to \tau^- \bar{\nu}_\tau)$ is expected to be $\simeq 0.5 \times 10^{-4}$ for $f_B = 190$ MeV and $|V_{ub}| = 0.003$. Nevertheless, in models with two Higgs doublets, it can be significantly larger due to the contribution of charged Higgs bosons [6]. The enhancement factor depends on the model parameters, in particular on the ratio of the vacuum expectation values for the Higgs fields, $\tan\beta$, and on the mass of the charged Higgs boson, $M_{H^\pm}$. No evidence for such an enhancement has been reported by experiments [7,8].

In this paper we present a measurement of $\mathcal{B}(D_s^- \to \tau^- \bar{\nu}_\tau)$ from the analysis of the fragmentation and decay chain $Z \to c\bar{c}$, $\bar{c} \to D_s^{*-}$ followed by $D_s^{*-} \to \gamma D_s^-$, $D_s^- \to \tau^- \bar{\nu}_\tau$, $\tau^- \to l^- \bar{\nu}_l \nu_\tau$. We also present the result of a search for $B^- \to \tau^- \bar{\nu}_\tau$.

2 Data Sample

The data were collected in 1994 by the L3 detector at LEP. The integrated luminosity is 49.6 pb^{-1} corresponding to a sample of 1,475,000 $Z \to q\bar{q}(\gamma)$ events at the centre of mass energy 91.2 GeV.

The L3 detector is described in Reference [9]. Briefly, the e^+e^- collision point is surrounded by a precision silicon vertex detector, a time-expansion tracking chamber, a high resolution electromagnetic calorimeter, a cylindrical shell of scintillation counters, a hadron calorimeter, and a muon chamber system. The detector is installed in a large solenoidal magnet providing a 0.5 Tesla field.

For the background study a Monte Carlo sample of 3,261,500 $e^+e^- \to Z(\gamma) \to q\bar{q}$ decays was generated with all quark flavours. For the efficiency studies 2500 $D_s^- \to \tau^- \bar{\nu}_\tau$ followed by $\tau^- \to l^- \bar{\nu}_l \nu_\tau$ decays and 1500 $B^- \to \tau^- \bar{\nu}_\tau$ decays were generated. The JETSET 7.4 Monte Carlo generator [10] was used to produce all these events. The Monte Carlo events are fully simulated in the L3 detector using the GEANT 3.15 program [11], which takes into account the effects of energy loss, multiple scattering and showering in the detector. The GHEISHA program [12] is used to simulate hadronic interactions in the detector materials.

[1)] The charge conjugate decays are understood to be included throughout the paper

The analysis is restricted to hadronic Z decays with $N_{tracks} > 7$ and with a large transverse energy imbalance ($E_\perp/E_{vis} > 0.25$). The number of events satisfying these preselection cuts is 33417. The sample consists mostly of $Z \to c\bar{c}$ (22.5%) and $Z \to b\bar{b}$ (66.2%) events where one of the leading heavy flavour hadrons decays semileptonically.

3 Reconstruction technique

To illustrate the reconstruction procedure, $D_s^- \to \tau^- \bar{\nu}_\tau$ decays followed by $\tau^- \to l^- \bar{\nu}_l \nu_\tau$ are considered. The signature of these decays is a lepton and large missing energy in one hemisphere of the event. For the reconstruction of $B^- \to \tau^- \bar{\nu}_\tau$ decays, a similar technique is used, with vertex requirements specific to B-meson decays.

The particle identification is done independently in the two hemispheres separated by a plane perpendicular to the thrust axis of the event. It is based upon the energy distribution in the electromagnetic and hadron calorimeters with respect to the trajectory of the charged track, as described in Reference [13]. The decay products of D_s^- comprise three neutrinos and a charged lepton. The energy and direction of the D_s^- is reconstructed using energy-momentum conservation:

$$\vec{P}_{D_s^-} = - \sum_{i \neq lepton} \vec{p}_i \quad (2)$$

$$E_{D_s^-} = \sqrt{s} - \sum_{i \neq lepton} E_i \, . \quad (3)$$

The summation is done over all detected particles in the event: charged and neutral hadrons, photons and leptons, except the lepton taken to be a τ decay product.

The energies of all reconstructed particles (E_i^{fit}) are then varied in the kinematic fit to minimise their combined deviations from the experimentally measured values

$$\chi^2 = \sum_{i \neq lepton} \frac{(E_i^{fit} - E_i^{meas})^2}{\sigma^2_{E_i^{meas}}}, \quad (4)$$

under the constraint $\sqrt{E^2_{D_s^-} - \vec{P}^2_{D_s^-}} = M_{D_s^-}$, where the fitted values are used in Equations 2-3. This procedure yields an energy resolution for the D_s^- mesons of about 3.0 GeV, slightly dependent on the energy, and an angular resolution of 60 mrad, as estimated using the Monte Carlo sample of $D_s^- \to \tau^- \bar{\nu}_\tau$ decays.

Extensive studies using a data sample of hadronic Z decays with high energy photons ($E_\gamma >$ 20 GeV) in the final state have been carried out to verify the detector performance. The identified photon is excluded from the reconstruction and its energy and direction are defined from the hadronic system using the constraint $E_\gamma = P_\gamma$ in the fit (Equation 4). The energy and angular resolutions estimated in this way are found to agree well (Fig. 1) between data and Monte Carlo.

4 Analysis of $D_s^- \to \tau^- \bar{\nu}_\tau$

Selection of the decay chain $D_s^{*-} \to \gamma D_s^-$, $D_s^- \to \tau^- \bar{\nu}_\tau$, $\tau^- \to l^- \bar{\nu}_l \nu_\tau$ requires a combination of lepton, photon and missing energy in one of the event hemispheres. Other particles in the same hemisphere are assumed to be fragmentation products and are used to reconstruct $E_{D_s^-}$

from the kinematic fit described in the previous section. The preselection described earlier leaves only 26% of the signal decays in the data sample under consideration. This is due to the transverse energy imbalance cut aimed to select hadronic events with high energy neutrinos.

Events are then selected with a well identified muon or electron in the least energetic event hemisphere. All the other tracks in the same hemisphere are required to point to the primary vertex within 3σ of the spatial resolution, in the plane perpendicular to the beam direction. The primary interaction point is not reconstructed on an event-by-event basis; the average beam position is used instead. The transverse size of the beam (ranging from 25 to 130 μm, depending on azimuthal angle) is accounted for in the definition of the spatial resolution.

The preselection cuts along with the requirement of a lepton in the less energetic hemisphere suppress to a negligible level the background from the decays $Z \to u\bar{u}$, $d\bar{d}$, $s\bar{s}$ and from hadronic decays of charm and beauty hadrons. However, the background from semileptonic decays is still very large. The requirement $E_{D_s^-} > 30$ GeV significantly suppresses semileptonic background, since the fitting procedure (Equation 4) substantially underestimates the momentum of heavy hadrons decaying semileptonically. This is due to hadronic decay products that are considered to come from the fragmentation. This requirement is one of the most important in the analysis, despite a significant loss in the signal selection efficiency which is estimated to be 7.3% at this stage. To eliminate misreconstructed signal and background events, the identified lepton is required to have a momentum in the D_s^- rest frame below 2 GeV.

Selected D_s^- candidates are then combined with photons in the same hemisphere. For the selected events the typical photon momentum from $D_s^{*-} \to \gamma D_s^-$ decays is harder than the momentum of photons from π^0 decays. In order to suppress the combinatorial background, the photon energy is required to be in the range from 3 GeV to 5 GeV. This cut significantly reduces the signal detection efficiency (to 2.0%), nevertheless it is vital to suppress the background which dominates at lower photon energies (Figure 2). In addition it is required that the photon must not form a π^0 with any other photon of energy greater than 0.1 GeV.

In semileptonic D decays, which constitute a significant fraction of the remaining background, the most energetic particle in the same hemisphere, with a charge opposite to that of the lepton, usually originates from the D decay. On average this particle is more energetic than fragmentation particles. Therefore, to suppress further the background from D semileptonic decays, the energy of the most energetic charged particle with a charge opposite to that of the lepton must be smaller than 3 GeV. The rejected background events show no excess in the signal region (Fig. 3). A typical candidate event for the decay chain $D_s^{*-} \to \gamma D_s^-$, $D_s^- \to \tau^- \bar{\nu}_\tau$, $\tau^- \to \mu^- \bar{\nu}_\mu \nu_\tau$ is presented in Figure 4.

The distribution of the $M(\gamma D_s^-)$ for the events satisfying the selection criteria is shown in Figure 5, along with the expected background and fitted signal. A binned maximum-likelihood fit is used to extract the number of $D_s^{*-} \to \gamma D_s^-$, $D_s^- \to \tau^- \bar{\nu}_\tau$ decays. The background shape and normalisation are fixed in the fit to the Monte Carlo prediction. In the peak region ($M(\gamma D_s^-) < 2.3$ GeV) there are 35 muon and 12 electron candidates in the data, in agreement with the Monte Carlo expectations (the efficiency for $\tau^- \to e^- \bar{\nu}_e \nu_\tau$ is 2.5 times lower than the efficiency for $\tau^- \to \mu^- \bar{\nu}_\mu \nu_\tau$). The invariant mass resolution is estimated to be 52 MeV/c^2 for the selected combinations of D_s^- and γ. There are several sources which contribute to the signal. The dominant one is $D_s^{*-} \to \gamma D_s^-$, $D_s^- \to \tau^- \bar{\nu}_\tau$; it amounts to 81% of the signal. The fit yields $N = 15.6 \pm 6.0$ for the number of these decays. The remaining 19% of the signal come from $D_s^{*-} \to \gamma D_s^-$, $D_s^- \to \mu^- \bar{\nu}_\mu$ decays as estimated from the partial decay width (Equation 1) and from the corresponding selection efficiency for this decay mode. A contribution from $D^{*-} \to D^- \pi^0/\gamma$, $D^- \to \mu^- \bar{\nu}_\mu$ and $D^- \to \tau^- \bar{\nu}_\tau$ is estimated to be negligible (0.16 decays using

Source		ΔN
Systematics	resolution function	1.6
	efficiency (statistics)	2.5
	efficiency (fragmentation)	1.6
	background (branching fractions)	0.5
	background (fragmentation)	0.6
	$\mathcal{B}(D_s^{*-} \to \pi^0 D_s^-)$	0.3
Subtotal	ΔN	3.4
Normalisation	D_s^*/D_s fraction	2.4
	D_s/c fraction	2.8
Subtotal	ΔN	3.7

Table 1: Summary of the systematic uncertainties in the fitted number ($N = 15.6 \pm 6.0$ (stat)) of signal decays.

Equation 1 and assuming $f_D = 250$ MeV).

Systematic errors on the number of signal decays arise from uncertainties in the detector resolution functions, background normalisation, the fragmentation functions and uncertainties in the D_s^*/D_s and D_s/c fractions. The uncertainty in the detector resolution function is estimated from the $Z \to q\bar{q}(\gamma)$ study (Fig. 1). The branching fractions of the most important background channels ($D \to \ell\nu_\ell K^0 X$) are varied according to the uncertainties in the PDG values for these decay modes [14]. The change in the c-quark fragmentation function ($< X_E^c >= 0.49 \pm 0.01$) affects signal efficiency and, to a lesser extent, background contamination. The uncertainty in the b quark fragmentation function ($< X_E^b >= 0.70 \pm 0.01$) contributes to the uncertainty in the background contamination.

The overall efficiency for the studied decays (the fragmentation process $\bar{c} \to D_s^{*-}$ followed by the decay sequence $D_s^{*-} \to \gamma D_s^-$, $D_s^- \to \tau^-\bar{\nu}_\tau$, $\tau^- \to l^-\bar{\nu}_l\nu_\tau$) is calculated to be $\eta = 0.017 \pm 0.003(stat)$ from the Monte Carlo simulation. It is reduced by $(4 \pm 2)\%$ to account for the measured branching fraction for the isospin violating decays $\mathcal{B}(D_s^{*-} \to \pi^0 D_s^-) = 0.062\ ^{+0.020}_{-0.018} \pm 0.022$ [15]. The Standard Model prediction for the branching fraction $\mathcal{B}(Z \to c\bar{c}) = 0.1724$ is used [16]. The branching fraction $\bar{c} \to D_s^{*-}$ is estimated to be 0.071 ± 0.017 in the analysis. This is based on the the fraction of D_s^- produced in the c-quark fragmentation, which is calculated to be 0.11 ± 0.02 from the measurements [17–20]; and on the fraction D_s^{*-}/D_s^-, which is estimated to be 0.65 ± 0.10 in agreement with the available indirect measurements [3, 21] and spin considerations. The latter two uncertainties are referred to as normalisation errors. A summary of the systematic errors is given in Table 1. When combining the systematic errors, all sources are assumed to be independent.

Finally, the branching fraction for $D_s^- \to \tau^-\bar{\nu}_\tau$ is determined to be

$$\mathcal{B}(D_s^- \to \tau^-\bar{\nu}_\tau) = (\ 7.4 \pm 2.8(\text{stat}) \pm 1.6(\text{syst}) \pm 1.8(\text{norm})\ )\ \%\ , \tag{5}$$

where the first error includes data and MC statistics, the second one represents experimental systematic uncertainties and the third one is due to normalisation uncertainties.

5 Search for $B^- \to \tau^- \bar{\nu}_\tau$

Selection of the fragmentation and decay chain $Z \to b\bar{b}$, $b \to B^- \to \tau^- \bar{\nu}_\tau$, $\tau^- \to X^- \nu_\tau$ is based on the following requirements: a track from τ decay that does not point to the primary vertex; low multiplicity in one event hemispheres and large missing energy.

First, a τ decay candidate is selected in the least energetic event hemisphere. The decay is identified by the presence of a lepton or hadron of at least 1 GeV momentum [13]. The associated track is required to be at least 4σ away from the primary vertex in the plane perpendicular to the beam direction. This particle is not used in the kinematic fit for the B^- energy and direction. The reconstructed energy of the B^- must exceed 30 GeV. This latter requirement significantly reduces the background from semileptonic decays.

All other tracks in the same hemisphere are required to have momenta smaller than 2 GeV and to be consistent with the primary vertex within 3σ in the transverse plane. In order to suppress background from the semileptonic decays involving K^0, which are not measured well and sometimes lead to a significant energy loss, no neutral hadron clusters with energy greater than 0.5 GeV are allowed in the 0.5 rad half-angle cone around the reconstructed B^- direction. In addition, events with extra identified leptons in the less energetic hemisphere are rejected.

The energy spectrum of the selected leptons is presented in Figure 6. The signal, corresponding to $\mathcal{B}(B^- \to \tau^- \bar{\nu}_\tau) = 10^{-3}$, is shown for illustration. The background shape (shaded area) is mostly due to the selection cuts, which require a very energetic B^- and low accompanying hadronic energy, and thus lead to preferential selection of high energy leptons from the semileptonic decays. On the other hand, for genuine $B^- \to \tau^- \bar{\nu}_\tau$ decays, the selection efficiency is fairly constant in the energy range from 1 to 10 GeV. It is important to note that due to the τ polarisation, $\mathcal{P}_\tau = +1$, in the $B^- \to \tau^- \bar{\nu}_\tau$ decays, leptons from τ decays are expected to populate preferentially the low energy region.

In the case of hadronic τ decays, further discrimination is required from the semileptonic background, which, at this point, consists mostly of semileptonic B decays with low energy leptons (<1GeV) and high energy neutrinos. Two additional variables are used to distinguish between signal and background. These variables are the invariant mass and energy of all the particles, except the τ decay product, in the 0.5 rad half-angle cone around the reconstructed B^- direction. Figure 7 shows the corresponding distributions. The cut on the invariant mass (<1.2 GeV) is indicated in Figure 7a.

The data agree with MC background expectations both for the leptonic and hadronic samples. The likelihood function, used to calculate the upper limit on the number of $B^- \to \tau^- \bar{\nu}_\tau$ decays, accounts for data and Monte Carlo statistics, and uses the data distributions presented in Figures 6 and 7b. The dependence of the likelihood function on the number of signal events is shown in Figure 8. The upper limit on the number of events due to the contribution from $B^- \to \tau^- \bar{\nu}_\tau$ decays is $N_{B^- \to \tau^- \bar{\nu}_\tau} < 3.8$ at 90% CL.

The overall efficiency for the studied decay is estimated to be $\eta = 0.028 \pm 0.005$ from Monte Carlo simulation. The branching fraction for $b \to B^-$ is taken to be 0.382 ± 0.025 [14]. Using the Standard Model prediction for the branching fraction $\mathcal{B}(Z \to b\bar{b}) = 0.2156$, the following upper limit is obtained

$$\mathcal{B}(B^- \to \tau^- \bar{\nu}_\tau) < 5.7 \times 10^{-4} \text{ at } 90\% \text{ CL} . \quad (6)$$

The analysis of the systematic uncertainties is similar to the one discussed in the previous section. An additional systematic error, which is due to the polarisation of τ leptons in $B^- \to \tau^- \bar{\nu}_\tau$ decays is estimated by reweighting the energy spectra of leptons and hadrons from τ

decays. The net effect is estimated to be small ($\sim 5\%$) since the efficiencies of the leptonic and hadronic channels are strongly anti-correlated.

6 Conclusion

A signal is observed in the invariant mass distribution $M(\gamma D_s^-)$, corresponding to the decay chain $D_s^{*-} \to \gamma D_s^-$, $D_s^- \to \tau^- \bar{\nu}_\tau$. The branching fraction is measured to be

$$\mathcal{B}(D_s^- \to \tau^- \bar{\nu}_\tau) = 0.074 \pm 0.028(\text{stat}) \pm 0.016(\text{syst}) \pm 0.018(\text{norm}) \ .$$

This allows a determination of the decay constant $f_{D_s^-}$

$$f_{D_s^-} = 309 \pm 58(\text{stat}) \pm 33(\text{syst}) \pm 38(\text{norm}) \text{ MeV} \ ,$$

using Equation 1 and the PDG values for $\tau_{D_s^-}$, $M_{D_s^-}$ and V_{cs} [14]. The first two errors are statistical and systematic and the third one represents the normalisation uncertainty due to the unknown branching fraction $c \to D_s^{*+}$. This result is compatible with other recent measurements of $f_{D_s^-}$ [2–5].

No evidence for $B^- \to \tau^- \bar{\nu}_\tau$ is seen in the data, yielding the upper limit

$$\mathcal{B}(B^- \to \tau^- \bar{\nu}_\tau) < 5.7 \times 10^{-4} \text{ at } 90\% \text{ CL} \ .$$

This result improves previously published limits [7,8].

Assuming $f_B = 190$ MeV and using $V_{ub} = 0.0033 \pm 0.0008$ [22], the following constraint is obtained:

$$\frac{\tan\beta}{M_{H^\pm}} < 0.38 \text{ at } 90\% \text{ CL}$$

This approaches the best limits on $\tan\beta$ and $M_{H^\pm}$ from the proton stability experiment [23] and from measurements of the $b \to s\gamma$ transition [24].

Acknowledgements

We wish to express our gratitude to the CERN accelerator divisions for the excellent performance of the LEP machine. We acknowledge the efforts of all engineers and technicians who have participated in the construction and maintenance of this experiment.

References

[1] J.Richman and P.Burchat, Rev.Mod.Phys. **67** (1995) 893.

[2] S.Aoki *et al.*, WA75 Collaboration, Prog.Theor.Phys.**89** (1993) 131.

[3] D.Acosta *et al.*, CLEO Collaboration, Phys.Rev. **D49** (1994) 5690;
D.Gibaut *et al.*, CLEO note CONF 95-22, June 1995.

[4] K.Kodama *et al.*, E653 Collaboration, preprint DPNU-96-33, June 1996.

[5] J.Z.Bai *et al.*, BES Collaboration, Phys.Rev.Lett **74** (1995) 4599.

[6] W.S.Hou, Phys.Rev. **D48** (1993) 2342.

[7] M.Artuso *et al.*, CLEO Collaboration, Phys.Rev.Lett. **75** (1995) 785.

[8] D. Buskulic *et al.*, ALEPH Collaboration, Phys.Lett. **B343** (1995) 444.

[9] L3 Collaboration, B.Adeva *et al.*, Nucl.Instr.Meth. **A289** (1990) 35;
J.A.Bakken *et al.*, Nucl.Instr.Meth. **A275** (1989) 81;
O.Adriani *et al.*, Nucl.Instr.Meth. **A302** (1991) 53;
K.Deiters *et al.*, Nucl.Instr.Meth. **A323** (1992) 162;
B.Acciari *et al.*, Nucl.Instr.Meth. **A351** (1994) 300.

[10] T.Sjöstrand and M.Bengtsson, Comp.Phys.Comm **43** (1987) 367;
T.Sjöstrand, CERN preprint, CERN-TH.6488/92.

[11] R. Brun *et al.*, preprint CERN DD/EE/84-1 (Revised 1987).

[12] H.Fesefeldt, RWTH Aachen Report PITHA 85/02 (1985).

[13] L3 Collaboration, M.Acciari *et al.*, Phys.Lett. **B341** (1994) 245;
M.Acciari *et al.*, Phys.Lett. **B352** (1995) 487.

[14] R.M.Barnett *et al.*, Particle Data Group Phys.Rev. **D54** (1996) 1.

[15] J.Gronberg *et al.*, CLEO Collaboration, Phys.Rev.Lett. **75** (1995) 3232.

[16] The LEP Experiments: ALEPH, DELPHI, L3, OPAL, *Electroweak Measurements and Constraints on the Standard Model*, preprint CERN-PPE/95-172.

[17] W.Y. Chen *et al.*, CLEO Collaboration, Phys.Lett. **B226** (1989) 192.

[18] H. Albrecht *et al.*, ARGUS Collaboration, Z.Phys. **C53** (1992) 361.

[19] D. Buskulic *et al.*, ALEPH Collaboration, Z.Phys. **C69** (1996) 585.

[20] G.Alexander *et al.*, OPAL Collaboration, preprint CERN-PPE/96-51, April 1996.

[21] D.Buskulic *et al.*, ALEPH Collaboration, Z.Phys. **C62** (1994) 1;
P.Abreu *et al.*, DELPHI Collaboration, Z.Phys. **C59** (1993) 533;
G.Alexander *et al.*, OPAL Collaboration, Z.Phys. **C67** (1995) 27.

[22] J.Alexander *et al.*, CLEO Collaboration, contribution to the 28th International Conference on High Energy Physics, ICHEP-96, PA05-081.

[23] J. Hisano, H. Murayama and T. Yanagida, Nucl.Phys. **B402** (1993) 46.

[24] M.S.Alam *et al.*, CLEO Collaboration, Phys.Rev.Lett. **74** (1995) 2885.

The L3 Collaboration:

M.Acciarri[28] O.Adriani[17] M.Aguilar-Benitez[27] S.Ahlen[11] B.Alpat[35] J.Alcaraz[27] G.Alemanni[23] J.Allaby[18] A.Aloisio[30] G.Alverson[12] M.G.Alviggi[30] G.Ambrosi[20] H.Anderhub[50] V.P.Andreev[39] T.Angelescu[13] F.Anselmo[9] D.Antreasyan[9] A.Arefiev[29] T.Azemoon[3] T.Aziz[10] P.Bagnaia[38] L.Baksay[45] R.C.Ball[3] S.Banerjee[10] K.Banicz[47] R.Barillère[18] L.Barone[38] P.Bartalini[35] A.Baschirotto[28] M.Basile[9] R.Battiston[35] A.Bay[23] F.Becattini[17] U.Becker[16] F.Behner[50] J.Berdugo[27] P.Berges[16] B.Bertucci[18] B.L.Betev[50] S.Bhattacharya[10] M.Biasini[18] A.Biland[50] G.M.Bilei[35] J.J.Blaising[18] S.C.Blyth[36] G.J.Bobbink[2] R.Bock[1] A.Böhm[1] B.Borgia[38] A.Boucham[4] D.Bourilkov[50] M.Bourquin[20] D.Boutigny[4] J.G.Branson[41] V.Brigljevic[50] I.C.Brock[36] A.Buffini[17] A.Buijs[46] J.D.Burger[16] W.J.Burger[20] J.Busenitz[45] X.D.Cai[16] M.Campanelli[50] M.Capell[16] G.Cara Romeo[9] M.Caria[35] G.Carlino[4] A.M.Cartacci[17] J.Casaus[27] G.Castellini[17] F.Cavallari[38] N.Cavallo[30] C.Cecchi[20] M.Cerrada[27] F.Cesaroni[24] M.Chamizo[27] A.Chan[52] Y.H.Chang[52] U.K.Chaturvedi[19] S.V.Chekanov[32] M.Chemarin[26] A.Chen[52] G.Chen[7] G.M.Chen[7] H.F.Chen[21] H.S.Chen[7] M.Chen[16] G.Chiefari[30] C.Y.Chien[5] M.T.Choi[44] L.Cifarelli[40] F.Cindolo[9] C.Civinini[17] I.Clare[16] R.Clare[16] H.O.Cohn[33] G.Coignet[4] A.P.Colijn[2] N.Colino[27] V.Commichau[1] S.Costantini[32] F.Cotorobai[13] B.de la Cruz[27] A.Csilling[14] T.S.Dai[16] R.D'Alessandro[17] R.de Asmundis[30] A.Degré[4] K.Deiters[48] P.Denes[37] F.DeNotaristefani[38] D.DiBitonto[45] M.Diemoz[38] D.van Dierendonck[2] F.Di Lodovico[50] C.Dionisi[38] M.Dittmar[50] A.Dominguez[41] A.Doria[30] I.Dorne[4] M.T.Dova[19,♯] E.Drago[30] D.Duchesneau[4] P.Duinker[2] I.Duran[42] S.Dutta[10] S.Easo[35] Yu.Efremenko[33] H.El Mamouni[26] A.Engler[36] F.J.Eppling[16] F.C.Erné[2] J.P.Ernenwein[26] P.Extermann[20] M.Fabre[48] R.Faccini[38] S.Falciano[38] A.Favara[17] J.Fay[26] O.Fedin[39] M.Felcini[50] B.Fenyi[45] T.Ferguson[36] D.Fernandez[27] F.Ferroni[38] H.Fesefeldt[1] E.Fiandrini[35] J.H.Field[20] F.Filthaut[36] P.H.Fisher[16] G.Forconi[16] L.Fredj[20] K.Freudenreich[50] C.Furetta[28] Yu.Galaktionov[29,16] S.N.Ganguli[10] P.Garcia-Abia[27] S.S.Gau[12] S.Gentile[38] J.Gerald[5] N.Gheordanescu[13] S.Giagu[38] S.Goldfarb[23] J.Goldstein[11] Z.F.Gong[21] A.Gougas[5] G.Gratta[34] M.W.Gruenewald[8] V.K.Gupta[37] A.Gurtu[10] L.J.Gutay[47] B.Hartmann[1] A.Hasan[31] D.Hatzifotiadou[9] T.Hebbeker[8] A.Hervé[18] W.C.van Hoek[32] H.Hofer[50] H.Hoorani[20] S.R.Hou[52] G.Hu[5] V.Innocente[18] H.Janssen[4] K.Jenkes[1] B.N.Jin[7] L.W.Jones[3] P.de Jong[18] I.Josa-Mutuberria[27] A.Kasser[23] R.A.Khan[19] D.Kamrad[49] Yu.Kamyshkov[33] J.S.Kapustinsky[25] Y.Karyotakis[4] M.Kaur[19,◇] M.N.Kienzle-Focacci[20] D.Kim[5] J.K.Kim[44] S.C.Kim[44] Y.G.Kim[44] W.W.Kinnison[25] A.Kirkby[34] D.Kirkby[34] J.Kirkby[18] D.Kiss[14] W.Kittel[32] A.Klimentov[16,29] A.C.König[32] I.Korolko[29] V.Koutsenko[16,29] R.W.Kraemer[36] W.Krenz[1] A.Kunin[16,29] P.Ladron de Guevara[27] G.Landi[17] C.Lapoint[16] K.Lassila-Perini[50] P.Laurikainen[22] M.Lebeau[18] A.Lebedev[16] P.Lebrun[26] P.Lecomte[50] P.Lecoq[18] P.Le Coultre[50] J.S.Lee[44] K.Y.Lee[44] C.Leggett[3] J.M.Le Goff[18] R.Leiste[49] E.Leonardi[38] P.Levtchenko[39] C.Li[21] E.Lieb[49] W.T.Lin[52] F.L.Linde[2,18] L.Lista[30] Z.A.Liu[7] W.Lohmann[49] E.Longo[38] W.Lu[34] Y.S.Lu[7] K.Lübelsmeyer[1] C.Luci[38] D.Luckey[16] L.Luminari[38] W.Lustermann[48] W.G.Ma[21] M.Maity[10] G.Majumder[10] L.Malgeri[38] A.Malinin[29] C.Maña[27] D.Mangeol[32] S.Mangla[10] P.Marchesini[50] A.Marin[11] J.P.Martin[26] F.Marzano[38] G.G.G.Massaro[2] D.McNally[18] S.Mele[30] L.Merola[30] M.Meschini[17] W.J.Metzger[32] M.von der Mey[1] Y.Mi[23] A.Mihul[13] A.J.W.van Mil[32] G.Mirabelli[38] J.Mnich[18] P.Molnar[8] B.Monteleoni[17] R.Moore[3] S.Morganti[38] T.Moulik[10] R.Mount[34] S.Müller[1] F.Muheim[20] A.J.M.Muijs[2] E.Nagy[14] S.Nahn[16] M.Napolitano[30] F.Nessi-Tedaldi[50] H.Newman[34] T.Niessen[1] A.Nippe[1] A.Nisati[38] H.Nowak[49] H.Opitz[1] G.Organtini[38] R.Ostonen[22] P.Pakhlov[29] D.Pandoulas[1] S.Paoletti[38] P.Paolucci[30] H.K.Park[36] G.Pascale[38] G.Passaleva[17] S.Patricelli[30] T.Paul[12] M.Pauluzzi[35] C.Paus[1] F.Pauss[50] D.Peach[18] Y.J.Pei[1] S.Pensotti[28] D.Perret-Gallix[4] B.Petersen[32] S.Petrak[8] A.Pevsner[5] D.Piccolo[30] M.Pieri[17] J.C.Pinto[36] P.A.Piroué[37] E.Pistolesi[28] V.Plyaskin[29] M.Pohl[50] V.Pojidaev[29,17] H.Postema[16] N.Produit[20] D.Prokofiev[39] G.Rahal-Callot[50] P.G.Rancoita[28] M.Rattaggi[28] G.Raven[41] P.Razis[31] K.Read[33] D.Ren[50] M.Rescigno[38] S.Reucroft[12] T.van Rhee[46] S.Riemann[49] K.Riles[3] O.Rind[3] S.Ro[44] A.Robohm[50] J.Rodin[16] F.J.Rodriguez[27] B.P.Roe[3] L.Romero[27] S.Rosier-Lees[4] Ph.Rosselet[23] W.van Rossum[46] S.Roth[1] J.A.Rubio[18] H.Rykaczewski[50] J.Salicio[18] E.Sanchez[27] M.P.Sanders[32] A.Santocchia[35] M.E.Sarakinos[22] S.Sarkar[10] M.Sassowsky[1] G.Sauvage[4] C.Schäfer[1] V.Schegelsky[39] S.Schmidt-Kaerst[1] D.Schmitz[1] P.Schmitz[1] M.Schneegans[4] N.Scholz[50] H.Schopper[51] D.J.Schotanus[32] J.Schwenke[1] G.Schwering[1] C.Sciacca[30] D.Sciarrino[20] J.C.Sens[52] L.Servoli[35] S.Shevchenko[34] N.Shivarov[43] V.Shoutko[29] J.Shukla[25] E.Shumilov[29] A.Shvorob[34] T.Siedenburg[1] D.Son[44] A.Sopczak[49] V.Soulimov[30] B.Smith[16] P.Spillantini[17] M.Steuer[16] D.P.Stickland[37] H.Stone[37] B.Stoyanov[43] A.Straessner[1] K.Strauch[15] K.Sudhakar[10] G.Sultanov[19] L.Z.Sun[21] G.F.Susinno[20] H.Suter[50] J.D.Swain[19] X.W.Tang[7] L.Tauscher[6] L.Taylor[12] Samuel C.C.Ting[16] S.M.Ting[16] M.Tonutti[1] S.C.Tonwar[10] J.Tóth[14] C.Tully[37] H.Tuchscherer[45] K.L.Tung[7] Y.Uchida[16] J.Ulbricht[50] U.Uwer[18] E.Valente[38] R.T.Van de Walle[32] G.Vesztergombi[14] I.Vetlitsky[29] G.Viertel[50] M.Vivargent[4] R.Völkert[49] H.Vogel[36] H.Vogt[49] I.Vorobiev[29] A.A.Vorobyov[39] A.Vorvolakos[31] M.Wadhwa[6] W.Wallraff[1] J.C.Wang[16] X.L.Wang[21] Z.M.Wang[21] A.Weber[1] F.Wittgenstein[18] S.X.Wu[19] S.Wynhoff[1] J.Xu[11] Z.Z.Xu[21] B.Z.Yang[21] C.G.Yang[7] X.Y.Yao[7] J.B.Ye[21] S.C.Yeh[52] J.M.You[36] An.Zalite[39] Yu.Zalite[39] P.Zemp[50] Y.Zeng[1] Z.Zhang[7] Z.P.Zhang[21] B.Zhou[11] Y.Zhou[3] G.Y.Zhu[7] R.Y.Zhu[34] A.Zichichi[9,18,19] F.Ziegler[49]

1 I. Physikalisches Institut, RWTH, D-52056 Aachen, FRG[§]
III. Physikalisches Institut, RWTH, D-52056 Aachen, FRG[§]
2 National Institute for High Energy Physics, NIKHEF, and University of Amsterdam, NL-1009 DB Amsterdam, The Netherlands
3 University of Michigan, Ann Arbor, MI 48109, USA
4 Laboratoire d'Annecy-le-Vieux de Physique des Particules, LAPP,IN2P3-CNRS, BP 110, F-74941 Annecy-le-Vieux CEDEX, France
5 Johns Hopkins University, Baltimore, MD 21218, USA
6 Institute of Physics, University of Basel, CH-4056 Basel, Switzerland
7 Institute of High Energy Physics, IHEP, 100039 Beijing, China[△]
8 Humboldt University, D-10099 Berlin, FRG[§]
9 INFN-Sezione di Bologna, I-40126 Bologna, Italy
10 Tata Institute of Fundamental Research, Bombay 400 005, India
11 Boston University, Boston, MA 02215, USA
12 Northeastern University, Boston, MA 02115, USA
13 Institute of Atomic Physics and University of Bucharest, R-76900 Bucharest, Romania
14 Central Research Institute for Physics of the Hungarian Academy of Sciences, H-1525 Budapest 114, Hungary[‡]
15 Harvard University, Cambridge, MA 02139, USA
16 Massachusetts Institute of Technology, Cambridge, MA 02139, USA
17 INFN Sezione di Firenze and University of Florence, I-50125 Florence, Italy
18 European Laboratory for Particle Physics, CERN, CH-1211 Geneva 23, Switzerland
19 World Laboratory, FBLJA Project, CH-1211 Geneva 23, Switzerland
20 University of Geneva, CH-1211 Geneva 4, Switzerland
21 Chinese University of Science and Technology, USTC, Hefei, Anhui 230 029, China[△]
22 SEFT, Research Institute for High Energy Physics, P.O. Box 9, SF-00014 Helsinki, Finland
23 University of Lausanne, CH-1015 Lausanne, Switzerland
24 INFN-Sezione di Lecce and Universitá Degli Studi di Lecce, I-73100 Lecce, Italy
25 Los Alamos National Laboratory, Los Alamos, NM 87544, USA
26 Institut de Physique Nucléaire de Lyon, IN2P3-CNRS,Université Claude Bernard, F-69622 Villeurbanne, France
27 Centro de Investigaciones Energeticas, Medioambientales y Tecnologicas, CIEMAT, E-28040 Madrid, Spain[♭]
28 INFN-Sezione di Milano, I-20133 Milan, Italy
29 Institute of Theoretical and Experimental Physics, ITEP, Moscow, Russia
30 INFN-Sezione di Napoli and University of Naples, I-80125 Naples, Italy
31 Department of Natural Sciences, University of Cyprus, Nicosia, Cyprus
32 University of Nijmegen and NIKHEF, NL-6525 ED Nijmegen, The Netherlands
33 Oak Ridge National Laboratory, Oak Ridge, TN 37831, USA
34 California Institute of Technology, Pasadena, CA 91125, USA
35 INFN-Sezione di Perugia and Universitá Degli Studi di Perugia, I-06100 Perugia, Italy
36 Carnegie Mellon University, Pittsburgh, PA 15213, USA
37 Princeton University, Princeton, NJ 08544, USA
38 INFN-Sezione di Roma and University of Rome, "La Sapienza", I-00185 Rome, Italy
39 Nuclear Physics Institute, St. Petersburg, Russia
40 University and INFN, Salerno, I-84100 Salerno, Italy
41 University of California, San Diego, CA 92093, USA
42 Dept. de Fisica de Particulas Elementales, Univ. de Santiago, E-15706 Santiago de Compostela, Spain
43 Bulgarian Academy of Sciences, Central Laboratory of Mechatronics and Instrumentation, BU-1113 Sofia, Bulgaria
44 Center for High Energy Physics, Korea Advanced Inst. of Sciences and Technology, 305-701 Taejon, Republic of Korea
45 University of Alabama, Tuscaloosa, AL 35486, USA
46 Utrecht University and NIKHEF, NL-3584 CB Utrecht, The Netherlands
47 Purdue University, West Lafayette, IN 47907, USA
48 Paul Scherrer Institut, PSI, CH-5232 Villigen, Switzerland
49 DESY-Institut für Hochenergiephysik, D-15738 Zeuthen, FRG
50 Eidgenössische Technische Hochschule, ETH Zürich, CH-8093 Zürich, Switzerland
51 University of Hamburg, D-22761 Hamburg, FRG
52 High Energy Physics Group, Taiwan, China

§ Supported by the German Bundesministerium für Bildung, Wissenschaft, Forschung und Technologie
‡ Supported by the Hungarian OTKA fund under contract number T14459.
♭ Supported also by the Comisión Interministerial de Ciencia y Technología
♯ Also supported by CONICET and Universidad Nacional de La Plata, CC 67, 1900 La Plata, Argentina
♢ Also supported by Panjab University, Chandigarh-160014, India
△ Supported by the National Natural Science Foundation of China.

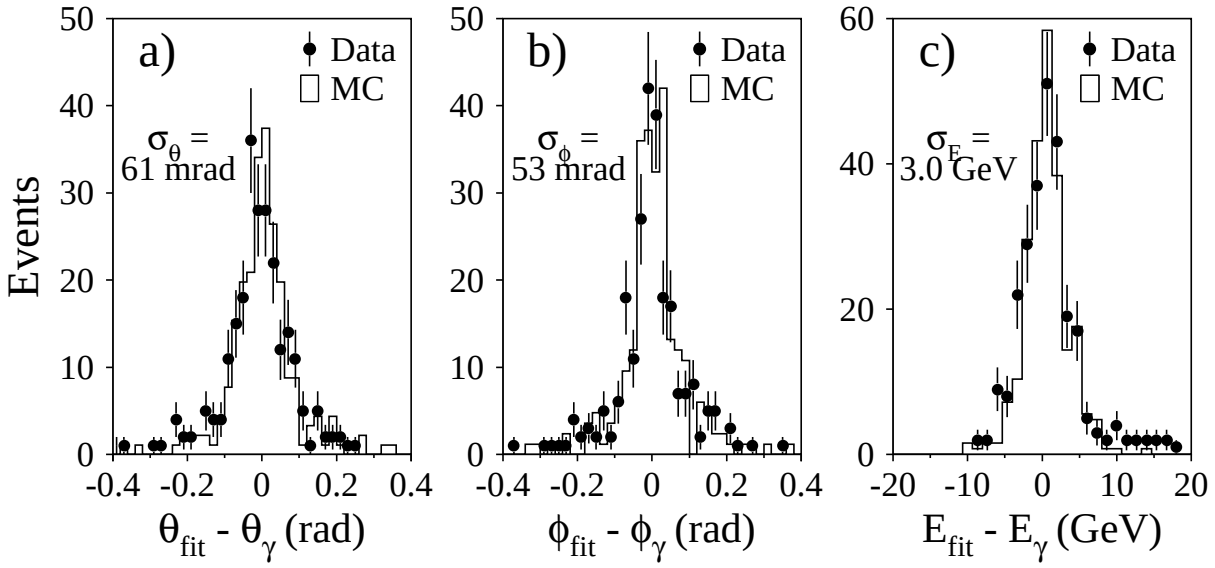

Figure 1: Study of the resolution functions using the control sample of $Z \to q\bar{q}(\gamma)$ events: a) polar angle resolution; b) azimuthal angle resolution; c) energy resolution. The quoted numbers correspond to the Gaussian fit.

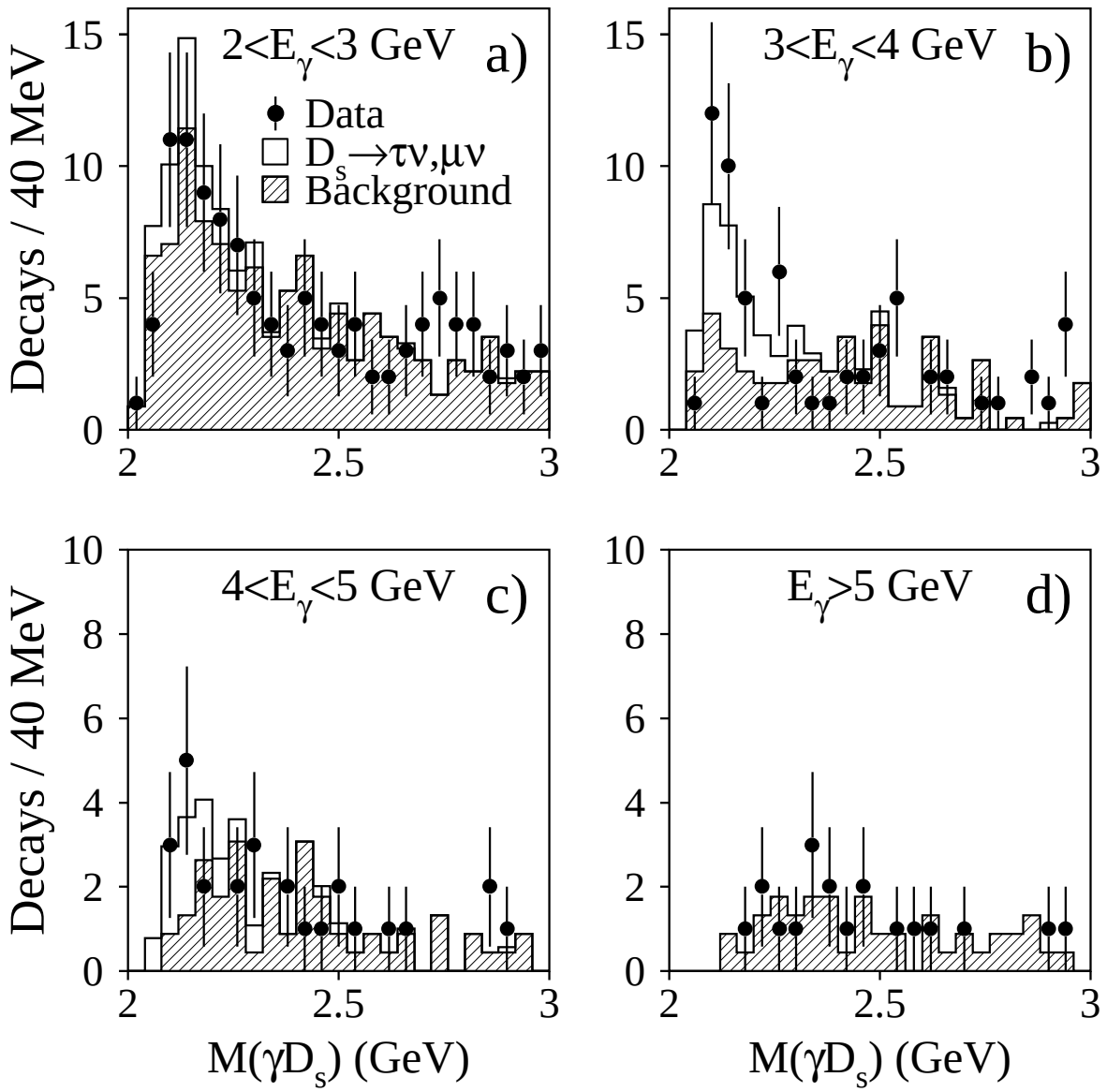

Figure 2: Invariant mass distributions, $M(\gamma D_s^-)$, for the different E_γ ranges.

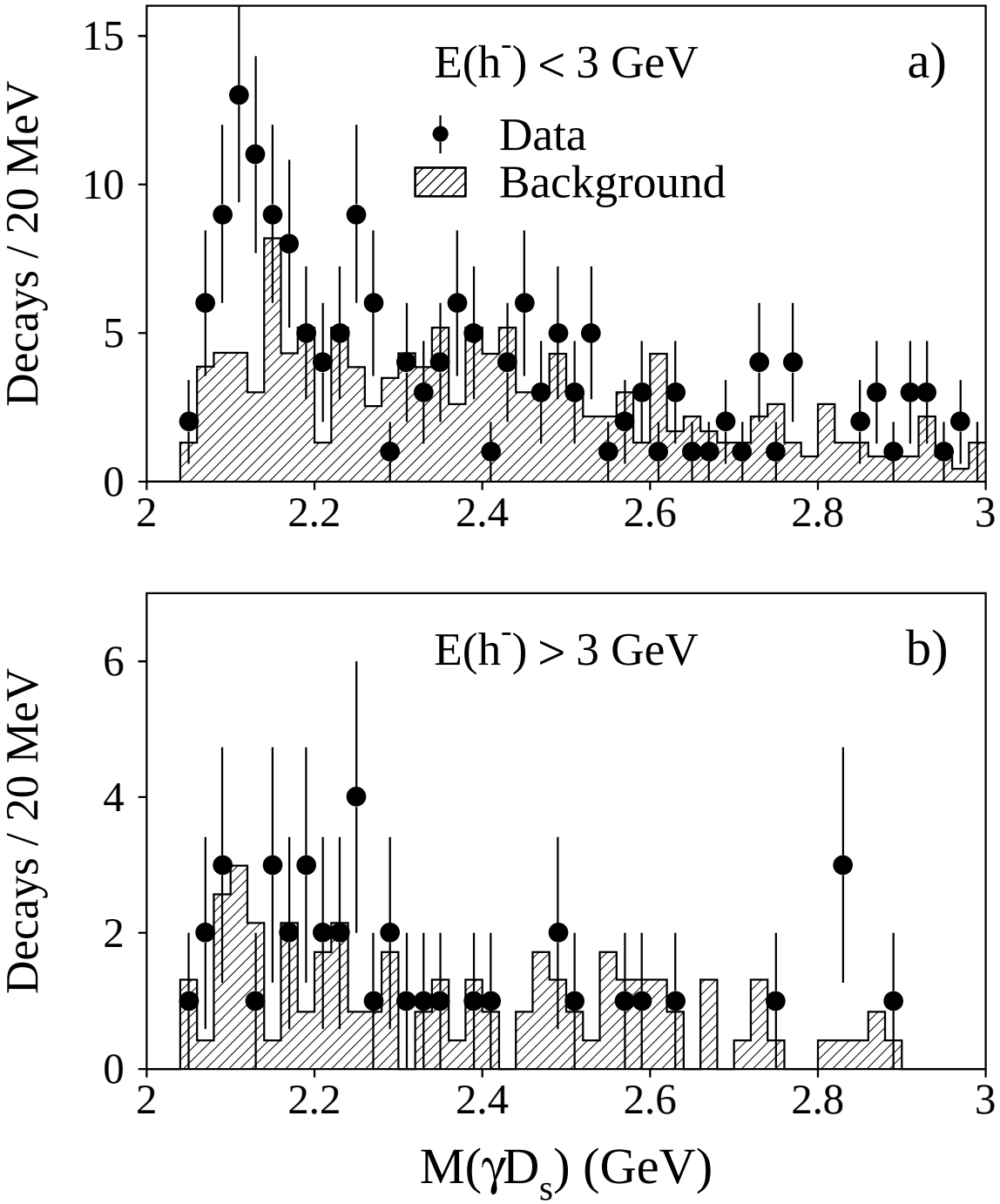

Figure 3: Invariant mass distributions, $M(\gamma D_s^-)$, for two data samples (a) and b)) corresponding to two energy ranges of the most energetic particle with a charge opposite to that of the lepton. Photon energy is required to exceed 2.5 GeV. The hatched histogram represents Monte Carlo estimates for the background.

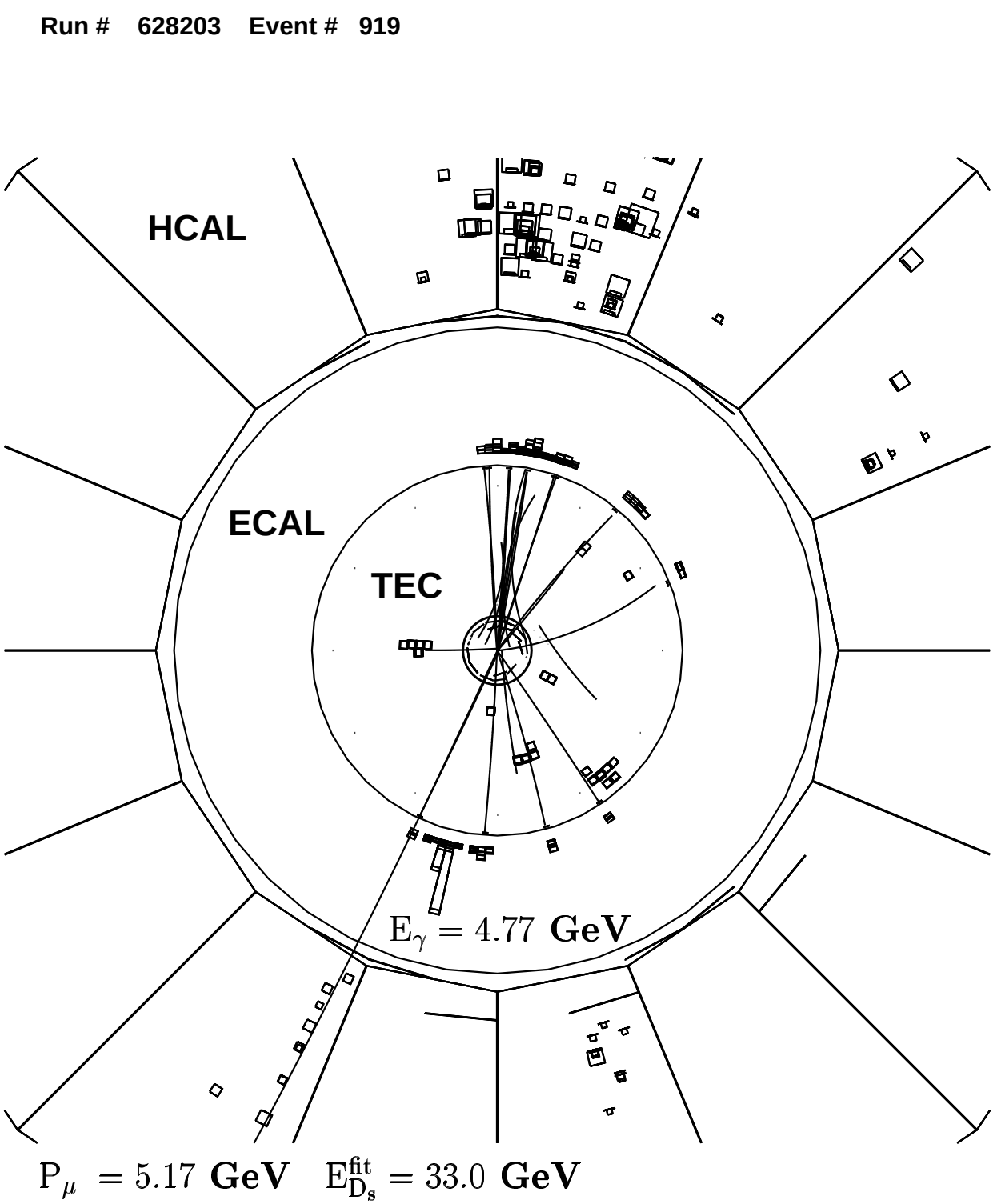

Figure 4: A candidate for the decay $D_s^{*-} \to \gamma D_s^-$, $D_s^- \to \tau^- \bar{\nu}_\tau$, $\tau^- \to \mu^- \bar{\nu}_\mu$. The invariant mass of the γD_s^- system is found to be $M(\gamma D_s^-) = 2.13$ GeV.

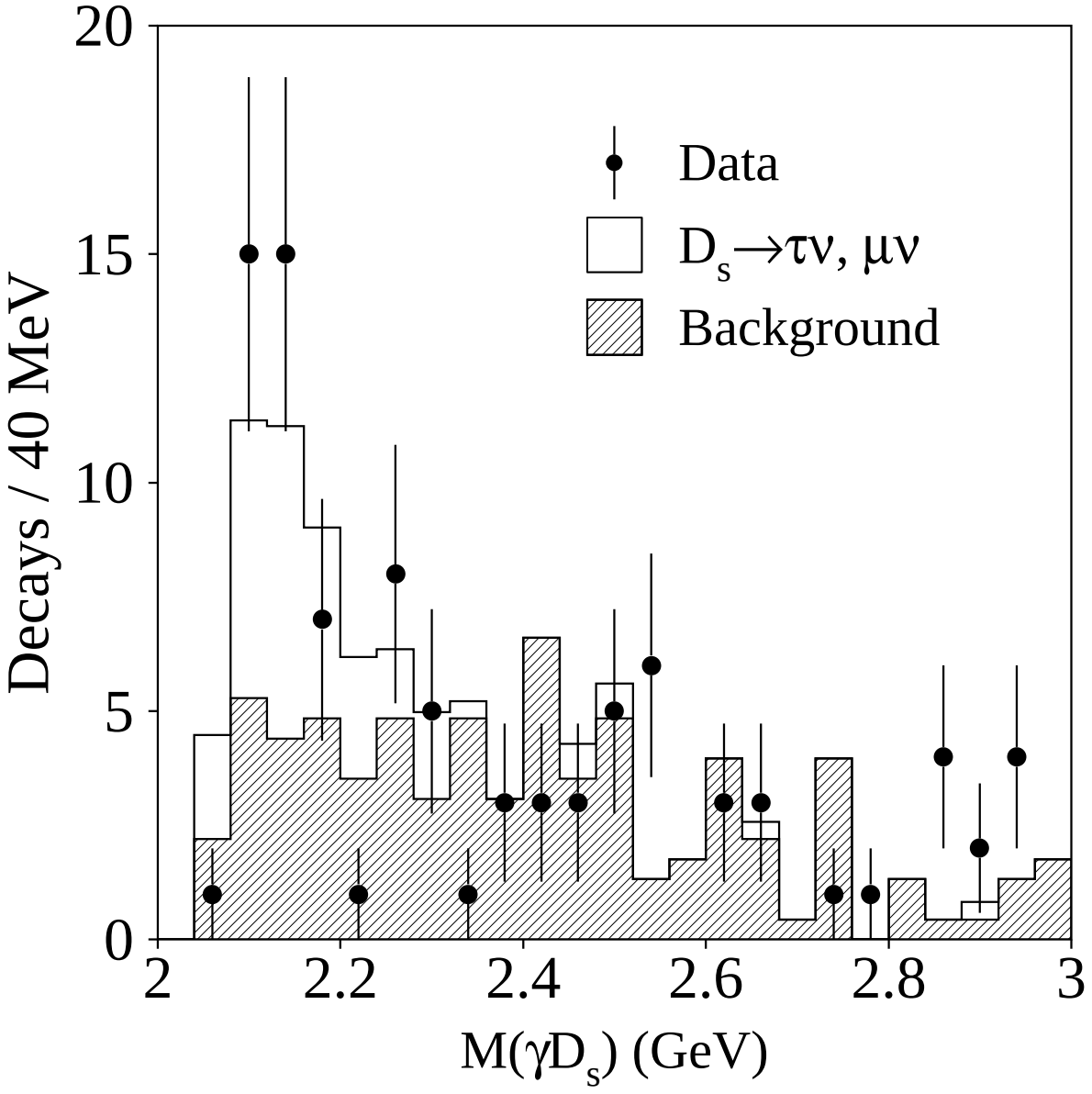

Figure 5: The invariant mass distribution, $M(\gamma D_s^-)$, for the selected events. The hatched histogram represents Monte Carlo estimates for the background, the open histogram shows the fitted signal.

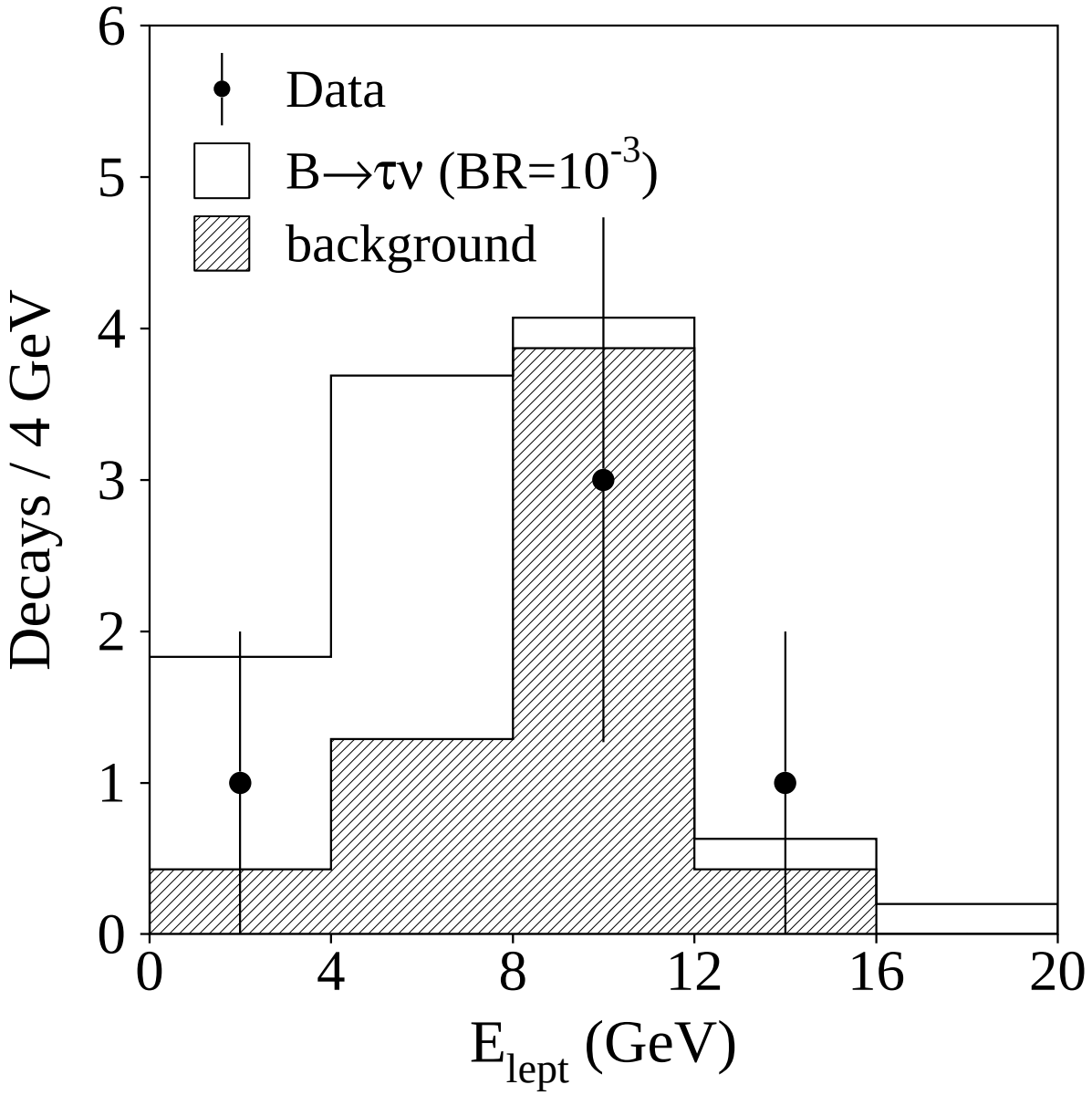

Figure 6: Lepton energy spectrum for the selected $B^- \to \tau^- \bar{\nu}_\tau$, $\tau^- \to l^- \bar{\nu}_l \nu_\tau$ candidates. The hatched histogram represents the background, the open histogram shows the signal contribution assuming $\mathcal{B}(B^- \to \tau^- \bar{\nu}_\tau) = 10^{-3}$.

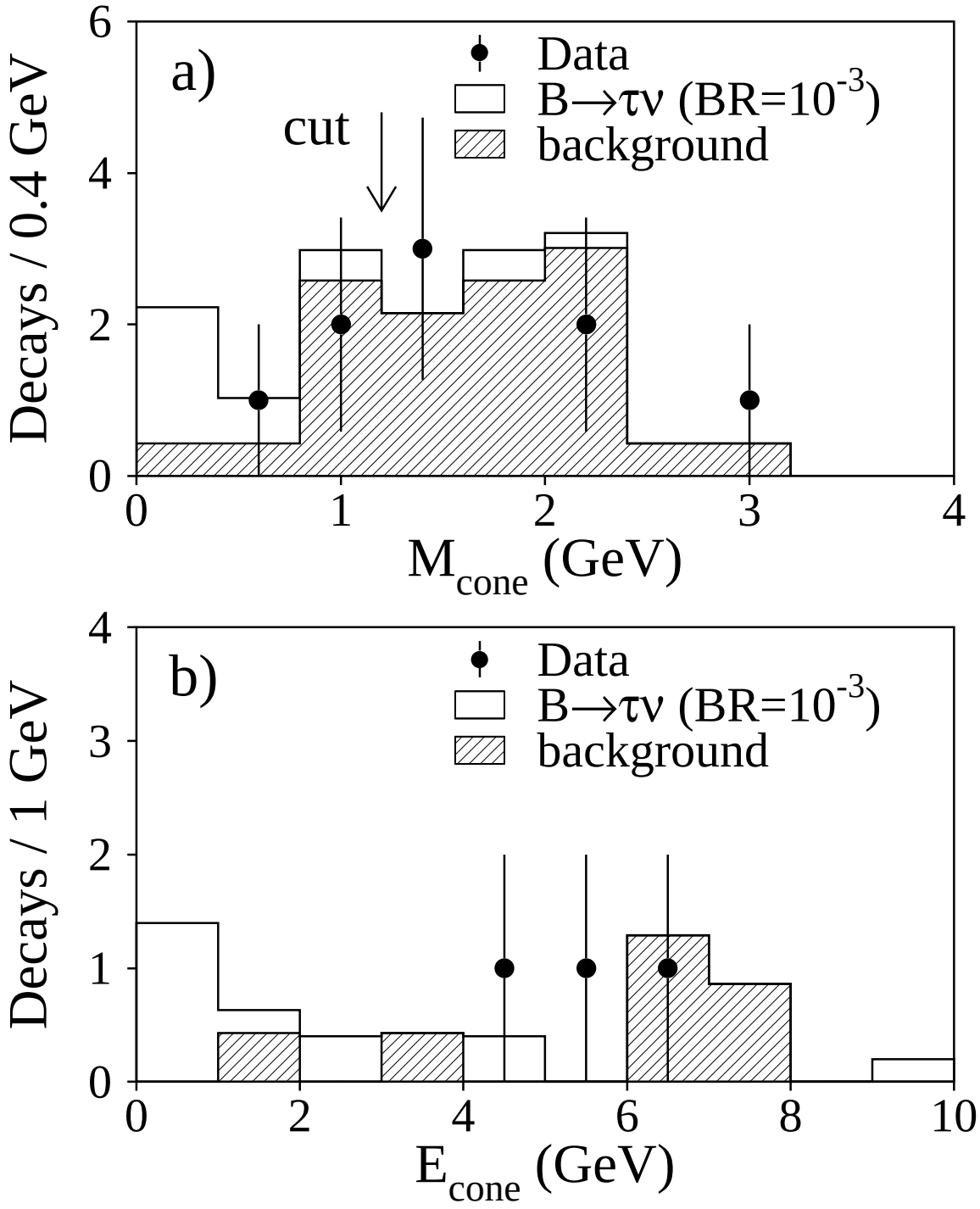

Figure 7: Selected candidates for the decay chain $B^- \to \tau^- \bar{\nu}_\tau$, $\tau^- \to \nu X_{\rm hadr}$. The distributions of the invariant mass (a) and total energy (b) for all particles, but identified charged tau decay product, in the 0.5 rad half-angle cone around the reconstructed B^- direction. The hatched histogram represents the background, the open histogram shows the signal contribution assuming $\mathcal{B}(B^- \to \tau^- \bar{\nu}_\tau) = 10^{-3}$. Figure 7b shows only events satisfying the cut indicated on Figure 7a.

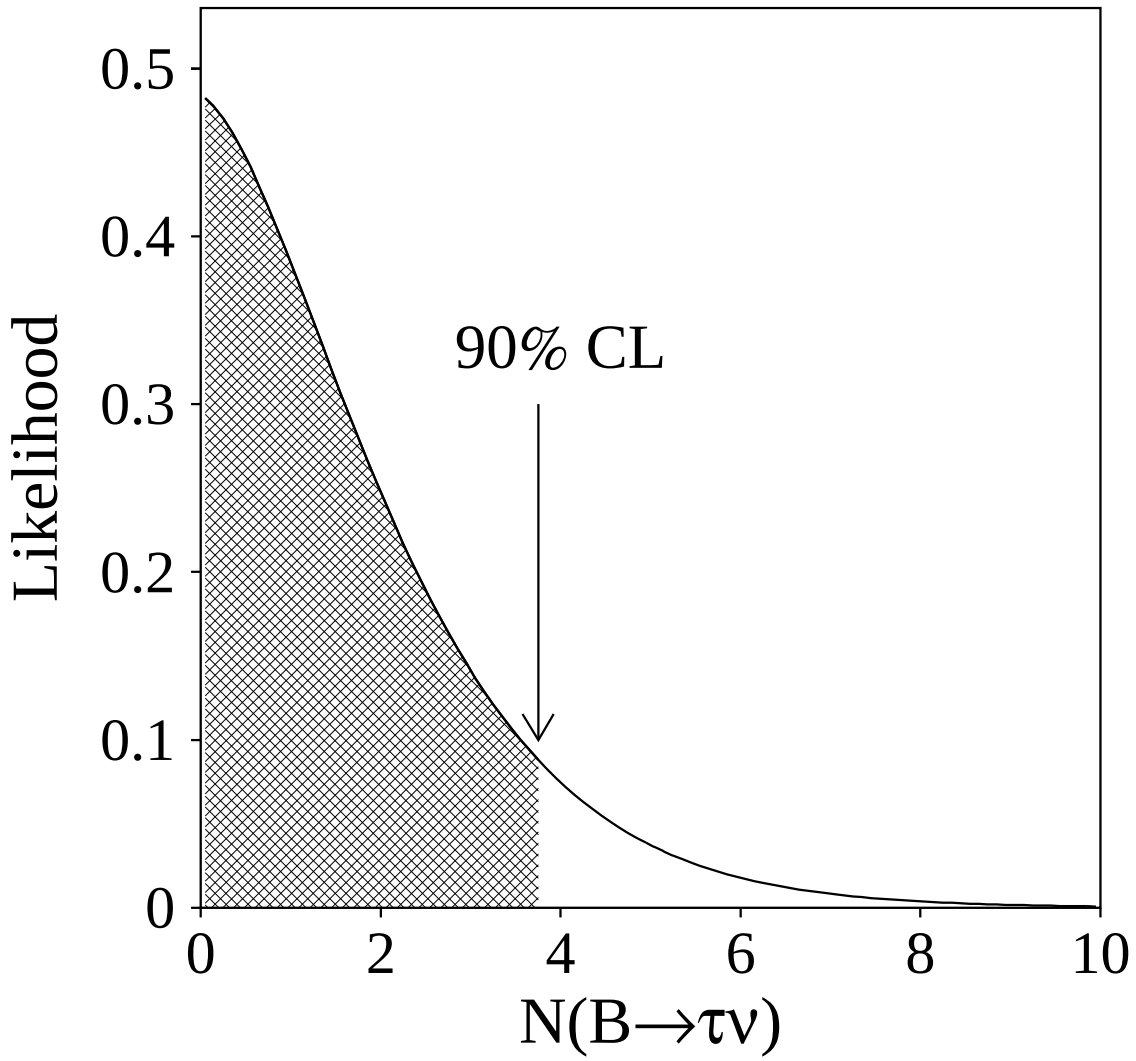

Figure 8: Probability density as a function of the number of $B^- \to \tau^- \bar{\nu}_\tau$ events. An upper limit at 90% confidence level corresponds to 3.8 events.